Applied Geochemistry 99 (2018) 1–1 2

Contents lists available at ScienceDirect

Applied Geochemistry

journal homepage: www.elsevier.com/locate/apgeochem

Using geochemistry to understand water sources and transit times in headwater streams of a temperate rainforest

Ian Cartwright[a,*], Alexander P. Atkinson[b], Benjamin S. Gilfedder[c], Harald Hofmann[d], Dioni I. Cendón[e], Uwe Morgenstern[f]

[a] School of Earth, Atmosphere and Environment, Monash University, Clayton, Vic, 3800, Australia [b] Marchment Hill Consulting, Melbourne, Vic, 3000, Australia [c] Limnological Research Station & Department of Hydrology, University of Bayreuth, Universitatsstrasse 30, 95447, Bayreuth, Germany [d] School of Civil Engineering & School of Earth and Environmental Science, The University of Queensland, St Lucia, Qld, 4072, Australia [e] Australian Nuclear Science and Technology Organisation, Institute for Environmental Research, Kirrawee DC, NSW, 2232, Australia [f] GNS Science, Lower Hutt, 5040, New Zealand

ARTICLEINFO

Editorial handling by Prof. M. Kersten

Keywords:
Tritium
Residence times
Macropores
Headwaters
Transit times

ABSTRACT

Understanding the sources and transit times of water that generates streamflow in headwater streams is important for understanding catchment functioning. This study determines the water sources and transit times in first-order streams from a temperate rainforest in the Otway Ranges, southeast Australia. Comparison of the major ion geochemistry of soil water, water flowing through soil pipes (macropores), and groundwater from the riparian zone adjacent to the stream suggests that water from soil pipes is the major contributor to streamflow. The tritium (^{3}H) activities of the stream water are between 1.80 and 2.06 TU, the water from the soil pipes has 3 3 H activities between 1.80 and 2.25 TU, the riparian zone groundwater has H activities of 1.35–2.39 TU, and one sample of soil water has a ^{3}H activity of 2.22 TU. These ^{3}H activities are significantly lower than those of local modern rainfall (2.6–3.0 TU), and mean transit times calculated using a range of lumped parameter models are between 3 and 57 years. These estimates are consistent with the major ion and stable isotope data, which imply that mean transit times were sufficiently long to allow weathering of minerals and/or organic matter and evapotranspiration to occur. The long mean transit times imply that water flows in this upper catchment are buffered against year-on-year variations in rainfall, but may change due to longer-term variations in rainfall or landuse.

1. Introduction

Documenting the sources of water that contribute to streamflow is important for understanding and managing catchments. Headwaters commonly contribute a significant proportion of total river flow (Alexander et al., 2007; Freeman et al., 2007; Meyer et al., 2007), with much of the water used downstream for agriculture, industry, or domestic supply originating in those areas. Because water from headwater catchments commonly has lower salinity and nutrient concentrations than lowland reaches, it is also important in maintaining river health. Lowland rivers typically traverse alluvial sediments, and groundwater inflows from those sediments may sustain streamflow during prolonged dry periods (Winter, 1995; Sophocleous, 2002; Tetzlaff and Soulsby, 2008). By contrast, the sources of water in headwater streams are less well understood. Despite being commonly developed on indurated or crystalline rocks that lack extensive groundwater systems (e.g., Lachassagne et al., 2011), many headwater streams are perennial. This implies that there must be long-lived stores of water in the catchment that can sustain streamflow during drier periods (Rice and Hornberger, 1998; Soulsby et al., 2005; Hrachowitz et al., 2010b, 2013; Morgenstern et al., 2010; Cartwright and Morgenstern, 2015, 2016a; Gusyev et al., 2016; Howcroft et al., 2018; Hofmann et al., 2018).

Clearing of native vegetation for agriculture, recreation, and human settlements is occurring in many headwater regions and these landscape modifications potentially change both recharge and runoff (e.g., Owuor et al., 2016). Climate change will also affect the amounts and distribution of rainfall in headwater catchments. Documenting the sources of water and timescales of water movement is important for understanding the potential impacts of these changes on headwater catchments. The volume of water stored in a catchment is proportional to the residence time and the rate of discharge (Maloszewski and Zuber, 1982). This results in catchments with limited water storage being vulnerable to short-term (months to years) changes in rainfall whereas catchments with larger storage capacity may be buffered against such variations. Additionally, anthropogenic activity may cause contamination of headwater areas, hence understanding the timescales of water movement is important for assessing the time lag between contamination occurring and those contaminants reaching the stream.

The increases in streamflow in response to rainfall represent the rate of pressure transmission through the subsurface, or the celerity of the system (van Verseveld et al., 2017; McDonnell and Beven, 2014). The pressure response of catchments is commonly rapid and streamflows may increase over a few hours following major rainfall events. However, the geochemistry of the stream water, even during the high streamflows following rainfall, is commonly dissimilar to that of recent rainfall (Sklash and Farvolden, 1979; Uhlenbrook et al., 2002; Botter et al., 2010; Cartwright and Morgenstern, 2018). Rather, the geochemical data are most consistent with water that is stored in the catchment being displaced by the infiltrating rainfall. This implies that the velocity of water flow is far lower than the celerity. Documenting both the physical response of streamflow to rainfall and the flow of water through the catchment is important for understanding catchment functioning.

* Corresponding author.
E-mail address: ian.cartwright@monash.edu (I. Cartwright).

https://doi.org/10.1016/j.apgeochem.2018.10.018
Received 10 May 2018; Received in revised form 20 September 2018; Accepted 22 October 2018 Available online 23 October 2018
0883-2927/

1.1. Sources and pathways of water

There are several potential stores of water in headwater catchments. These include shallow relatively young water stores such as surface runoff, soil water, and interflow and the underlying groundwater, which is likely to be older. Mineral dissolution in the soils and aquifers increases the concentrations of silica, the major cations, and some anions, notably bicarbonate and sulfate (Uhlenbrook and Hoeg, 2003; Hugenschmidt et al., 2014; Cartwright et al., 2018; Hofmann et al., 2018). The breakdown of organic material in soils increases the concentrations of dissolved inorganic and organic carbon and nitrate in soil water. Evapotranspiration, which is important in arid and semi-arid regions, increases the concentrations of all major ions. Thus, groundwater and soil water almost invariably has higher concentrations of most major ions than rainfall (Herczeg and Edmunds, 2000; Edmunds, 2009). The variable operation of these processes may also result in the different stores of water having different major ion geochemistry. For example, due to the abundance of organic matter, soil water commonly has higher nitrate concentrations than groundwater.

A significant volume of the water in steep temperate forested catchments may enter the streams via preferential flow paths or macropores (McDonnell, 1990; Jones, 1997, 2004; Uchida et al., 1999). Preferential flow may occur through fractures in the bedrock, locally saturated zones at the soil-bedrock interface, and soil pipes. The latter commonly occur at the soil-bedrock interface and are water-sculpted erosional features formed by concentration of subsurface flow along features such as decaying tree roots, fractures, or zones of locally higher hydraulic conductivity (Jones, 1997, 2004). Soil pipes have been documented in numerous steep high-rainfall headwater catchments, for example in Plynlimon, Wales (Jones, 1997, 2004), Tama, Japan (Uchida et al., 1999, 2005), British Columbia, Canada (Anderson et al., 2009), and Victoria and New South Wales, Australia (Crouch et al., 1986; Boucher and Powell, 1994). Soil pipes are the largest of the macropores, commonly reaching several tens of centimetres diameter, and they can form metre-to hundreds of metre-scale networks that may channel subsurface flow of water derived from large areas.

1.2. Timescales of water movement

The transit time (also commonly referred to as the residence time) is the time taken for water to pass through a catchment from where it infiltrates to where it discharges into a stream or is sampled from within the aquifers or soils (McGuire and McDonnell, 2006). The flow paths of water through the unsaturated or saturated zones commonly have varying lengths, and thus the water sampled from a stream or aquifer has a distribution of transit times rather than a discrete age. Even if flow paths are close to being parallel (e.g., in a confined aquifer), macroscopic dispersion produces a distribution of transit times (e.g., Maloszewski and Zuber, 1982; McGuire and McDonnell, 2006). Lumped parameter models may be used to estimate the mean and distribution of transit times and tracer concentrations in aquifers with homogeneous hydraulic properties, simplified geometries, and uniform recharge rates (Maloszewski and Zuber, 1982; Maloszewski, 2000; Zuber et al., 2005; McGuire and McDonnell, 2006).

The attenuation of stable isotope ratios or major ion concentrations between rainfall and catchment waters are commonly used to calculate mean transit times (e.g., McGuire and McDonnell, 2006). However, these tracers become ineffective where transit times are in excess of 4–5 years as the temporal variations are smoothed out (Stewart et al., 2010). Because the typical mean transit times in most Australian headwater catchments are >10 years (Cartwright and Morgenstern, 2015, 2016a; 2016b, 2018; Duvert et al., 2016; Cartwright et al., 2018; Howcroft et al., 2018; Hofmann et al., 2018), it is not generally possible to use stable isotopes or major ions to estimate transit times.

Tritium (^{3}H) has half-life of 12.32 years and may be used to estimate mean transit times via lumped parameter models where these are < 150 years (Clark and Fritz, 1997; Morgenstern et al., 2010). ^{3}H is part of the water molecule and, unlike radioactive tracers such as ^{14}C, its concentration is little affected by geochemical or biogeochemical reactions in the soils or aquifer matrix (although minor retardation in clay-rich soils may occur: Furuichi et al., 2016). Additionally, unlike the gas tracers (e.g. ^{3}He, SF_6, and the chlorofluorocarbons), ^{3}H does not exchange with the atmosphere or degas. Thus, ^{3}H may be used to estimate transit times of surface water, water from the unsaturated zone, or groundwater; and those transit times reflect the time taken for the water to flow through both the unsaturated and saturated zones. Due to the production of ^{3}H in atmospheric thermonuclear tests, rainfall ^{3}H activities peaked in the 1950s–1960s (the ^{3}H "bomb-pulse"). The ^{3}H

activities of remnant bomb-pulse waters in the Southern Hemisphere are now below those of modern rainfall (Morgenstern et al., 2010; Tadros et al., 2014), mean transit times may be estimated from individual ^{3}H activities rather than requiring time-series measurements of catchment waters as is the case in the Northern Hemisphere (Morgenstern et al., 2010). However, the diminishing of the bomb pulse ^{3}H means that it is not feasible to test the suitability of lumped parameter models using time-series data that commence now. Rather a suitable lumped parameter model needs to be adopted based on the knowledge of the geometry of the flow system or previous time-series studies in similar catchments.

Not being able to assess the suitability of the lumped parameter model represents an uncertainty in the mean transit times. Other uncertainties arise from uncertainties in the ^{3}H activity of rainfall, whether seasonal recharge occurs, and the effects of macroscopic mixing caused by water following different flow paths (aggregation) (McCallum et al., 2014; Suckow, 2014; Cartwright and Morgenstern, 2015, 2016a; 2016b; Kirchner, 2016). However, the decline of the bomb-pulse ^{3}H activities in the Southern Hemisphere results in the ^{3}H activities of catchment waters being proportional to the mean transit times (i.e. water with low ^{3}H activities have longer mean transit times than water from the same location with higher ^{3}H activities). This allows relative transit times to be determined, which in itself is useful in understanding catchment functioning.

As noted above, the mean transit times in Australian headwater catchments are commonly years to decades, which are significantly longer than those in many similar catchments globally (McGuire and McDonnell, 2006; Stewart et al., 2010). The long mean transit times may result from high evapotranspiration rates of the native Australian vegetation that limits groundwater recharge. Additionally, the vast

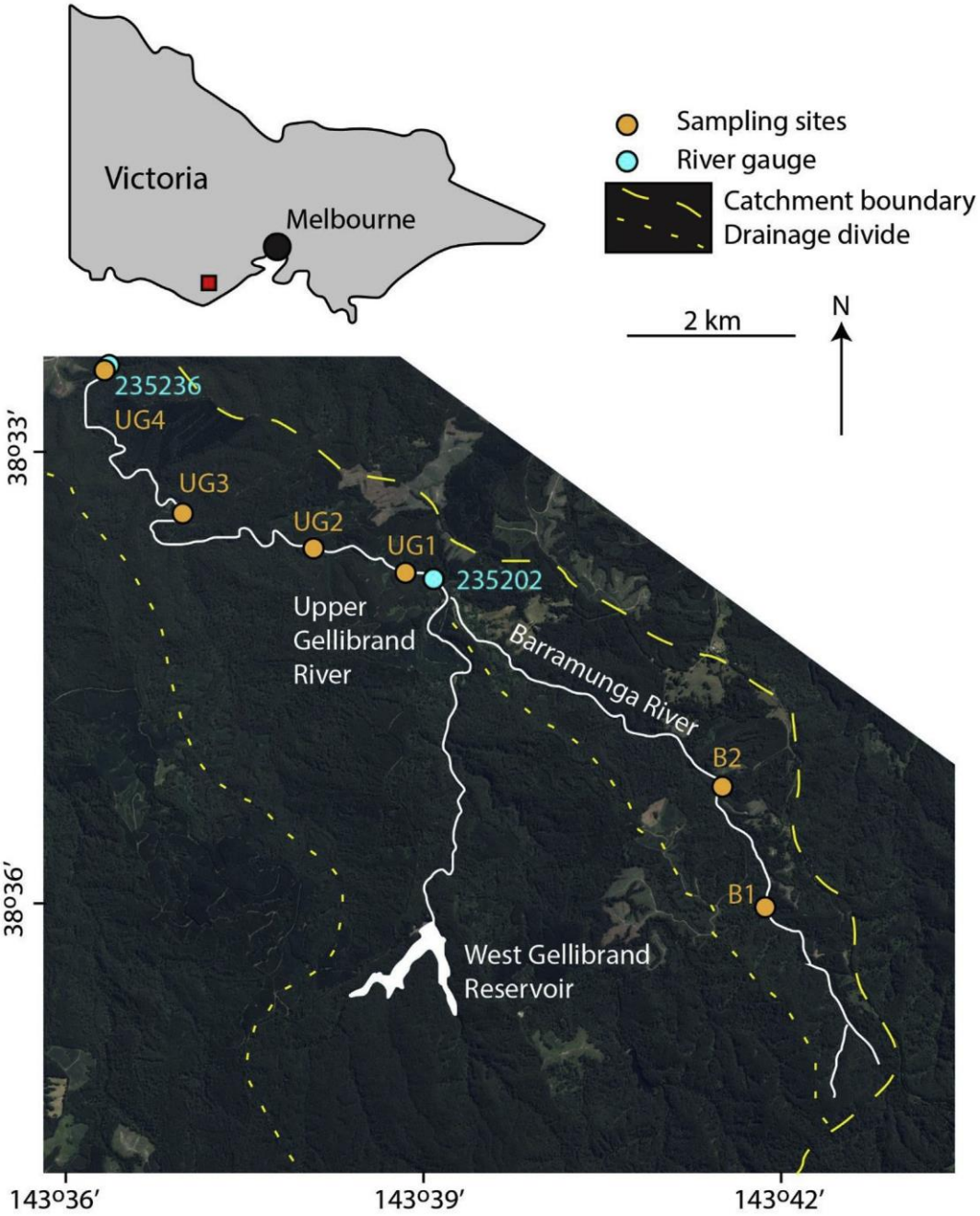

Fig. 1. Google Earth® image of the study area showing the boundary of the Gellibrand Catchment, drainage divides (sub-catchment boundaries) of tributaries within the Gellibrand Catchment, and sampling sites. Catchment boundaries were constrained using the topography. River gauges are maintained by the Victoria State Government Department of Environment, Land, Water and Planning. Inset shows location of study area in Victoria.

majority of mainland Australia was not glaciated, and the regolith has high storage volumes due to it being deeply weathered. These long mean transit times imply that water may be held in transient stores such as the soil or interflow for several years before being mobilised.

1.3. Objectives

This study is based in the headwaters of the Gellibrand River in southwest Victoria (Fig. 1). It tests the following hypotheses. Firstly, that major ion and stable isotope geochemistry may be used to discriminate between the relative contribution of macropore flow, shallow riparian groundwater, and water from the soils to streamflow. Secondly, that the water stores have transit times of several years. While this study is based on a specific example, it has broad general implications for understanding headwater catchments in general, in particular for assessing the timescales of change of water quality and the volumes of water in storage. Notably, in contrast to groundwater and stream water, estimates of transit times of soil water and water discharging from the soils or regolith via macropores are limited (e.g., Kabeya et al., 2007; Lee et al., 2007; Zhang et al., 2017). However, documenting the timescales of water movement in the soils and regolith are important in understanding catchment resilience and the volume of water held in storage.

2. Study area

Part of the headwaters of the Gellibrand River (Fig. 1) occur on the northwest slopes of the Otway Ranges in southwest Victoria (Atkinson et al., 2014, 2015). This section of the upper Gellibrand catchment has steeply incised river valleys dominated by wet sclerophyll forest with native vegetation dominated by Mountain Ash (Eucalyptus regans) with an understory comprising Acaias (typically Acacia melanoxylon, A. verticillata, and A. stricta), tree-ferns (Cyathea australis and Dicksonia antarctica) and numerous species of ferns, sedges, and grasses (Parks Victoria, 2018). The upper Gellibrand River upstream of gauge 253236 (Fig. 1), which is currently inactive, has a catchment area of ~80 km^2 and occurs at elevations of between 100 and 550 m AHD (Australian Height Datum: Department of Environment, Land, Water and Planning, 2018). The Barramunga River is an ungauged tributary of the upper Gellibrand River with a catchment area of ~16 km^2 (Department of Environment, Land, Water and Planning, 2018). Average rainfall is between 1000 and 1200 mm/year with the austral winter months having higher rainfall totals (Bureau of Meteorology, 2018).

Between 2000 and 2017, the streamflow at gauge 235202 on the Gellibrand River ranged from 1.0×10^3 to 4.1×10^6 m^3/day with higher streamflows in winter (Department of Environment, Land, Water and Planning, 2018). Annual streamflows during this period were between 9.2×10^6 and 3.8×10^7 m^3 (average of 2.3×10^7 m^3). The West Gellibrand Reservoir has a capacity of 1.8×10^6 m^3 and is used for local domestic water supply. The discharge of water from this storage mimics the natural flows and has little impact on the flows in the upper catchment (Williams, 2004). Because the streams are deeply incised and perennial, it is most likely that they are gaining. This conclusion is consistent with ^{222}Rn activities of stream water in the upper catchment that are up to 600 Bq/m^3 (Atkinson, 2014).

The riparian zone is up to a few metres wide. It consists of poorly sorted sediments that range in grain size between clay and cobbles. The streambed commonly comprises a layer of fine-grained organic- and clay-rich mud that is typically a few centimetres to tens of centimetres thick that overlies the coarser-grained sediments. The bedrock comprises indurated siltstones, mudstones, and sandstones of the Cretaceous Eumarella Formation (Atkinson et al., 2014, 2015). These rocks are typically weathered to depths of between 3 and 10 m close to the present-day land surface and host groundwater flow in the weathered zone and fractures. Locally, layers of saprolitic clay are present. The main soils are dermosols (Australian Soil Resource Information System, 2018) that based on field observations are locally at least 2 m thick. The soils have a 20–30 cm thick surficial organic layer overlying a 20–30 cm thick sandy loam A horizon and a B horizon with medium to high clay contents. Soil pipes draining the lower parts of the soil profile or the upper parts of the regolith were observed in stream banks throughout the Barramunga subcatchment. The soil pipes have diameters of up to 50 cm (although most are <30 cm). Some of the soil pipes were flowing constantly through the study period, whereas others are ephemeral and ceased flowing during the summer months. Gullies formed from collapsed pipes were traceable for distances of metres to tens of metres on the hill slopes.

3. Methods

3.1. Field sampling

Sampling took place from four sites in the upper Gellibrand and two sites in the Barramunga Rivers (Fig. 1) between September 2011 and August 2013 (Table S1). A total of 12 sampling campaigns were conducted that encompass all seasons, although not all sites were sampled in each campaign. Water from the streams was sampled from the centre of swiftly flowing reaches using an open container. Eleven 80 mm diameter PVC piezometers with screens of 10–20 cm located 0.5–1 m below the water table were installed in the riparian zones within 5 m of the streams. Water from the piezometers was sampled using a bailer; in excess of three bore volumes were extracted prior to sampling. Soil water was extracted using UMS SIC20 suction lysimeters with 60 mm long 20 mm diameter silicon-carbide cups installed at depths of approximately 20, 50, and 90 cm at B2 and UG3. The water samples were extracted into sealed evacuated bottles (max. vacuum −80 kPa). The systems remained in place for several weeks and observations made in the laboratory indicate that they typically sample water for several days before the vacuum degrades. Flow from a perennial soil pipe (SP1 at locality B1) was measured via a V-notch weir constructed from a plastic tank into which the pipe flow was guided. The notch angle was 12.5° and flow was estimated from the depth of water in the tank measured at 30 min intervals using a Winsitu Aqua Troll 200 logger corrected for barometric pressure using a co-located Winsitu Barotroll logger. The depth vs. flow relationship was calibrated in the laboratory at flow rates of up to 100 m^3/day (R^2 =0.96). Salt gauging following Kite (1989) was used to estimate streamflow in the Barramunga River. Streamflow in the upper Gellibrand River at gauge 2235202 (Fig. 1) is from the Department of Environment, Land, Water and Planning (2018). The nearest rainfall station is at Forrest, ~6 km northeast of the study area (Bureau of Meteorology, 2018).

3.2. Geochemical analyses

Geochemical analyses were carried out as in previous studies (e.g., Cartwright and Morgenstern, 2015, 2018; Atkinson et al., 2015; Howcroft et al., 2018). EC values were measured in the field using a calibrated TPS meter and probe. HCO_3 concentrations were measured on a subset of samples within 12 h of sample collection using a Hach digital titrator and reagents and are precise to ±5%. Major ions were measured at Monash University. Anion concentrations were determined

on filtered unacidified samples using a Metrohm ion chromatograph. Cation concentrations were determined on filtered samples that had been acidified to pH < 2 with ultrapure 16N HNO_3 and analysed on a ThermoFinnigan X series Quadrupole ICP-MS. The precision of the major ion analyses based on replicate analyses is ±2% and accuracy based on the analysis of certified standards is ± 5%. A complete set of major ion analyses were made on ~50% of the samples and charge balances for these are within ±5%.

Stable isotope ratios were measured at Monash University using Finnigan MAT 252 and ThermoFinnigan DeltaPlus Advantage mass spectrometers. δ^2H values were measured via reaction with Cr at 850 °C in a Finnigan MAT H/Device and $\delta^{18}O$ values were measured via equilibration with $HeeCO_2$ at 32 °C in a ThermoFinnigan Gas Bench. δ_2H and $\delta_{18}O$ values were normalised against internal standards calibrated using SMOW, GISP, and SLAP following Coplen (1988) and are expressed in per mil (‰) relative to V-SMOW. Precision (σ) based on replicate analyses is ±0.2‰ for $\delta^{18}O$ and ±1‰ for δ^2H. Tritium activities were measured at either the Australian Nuclear Science and Technology Organisation (ANSTO), Sydney, or the Institute of Geological and Nuclear Sciences (GNS), Lower Hutt. Samples for ^3H were distilled and electrolytically enriched prior to being analysed by liquid scintillation as described by Neklapilova (2008a, 2008b) and Morgenstern and Taylor (2009). ^3H activities are expressed in Tritium Units (TU). At the time of analysis, typical relative uncertainties and quantification limits were ±5% and 0.13 TU at ANSTO and ±2% and
0.02 TU at GNS.

3.3. Principle components analysis

Similarity in major ion concentrations were assessed by principle component analysis (PCA) (Menció et al., 2012) using the IBM SPSS Statistics 25 computer program. Concentrations of Cl, NO_3, SO_4, Na, K, Mg, and Ca were considered in all samples where these ions were measured. Since HCO_3 concentrations were not measured on all samples (Table S1) they were not considered in the analysis. The Kaiser-

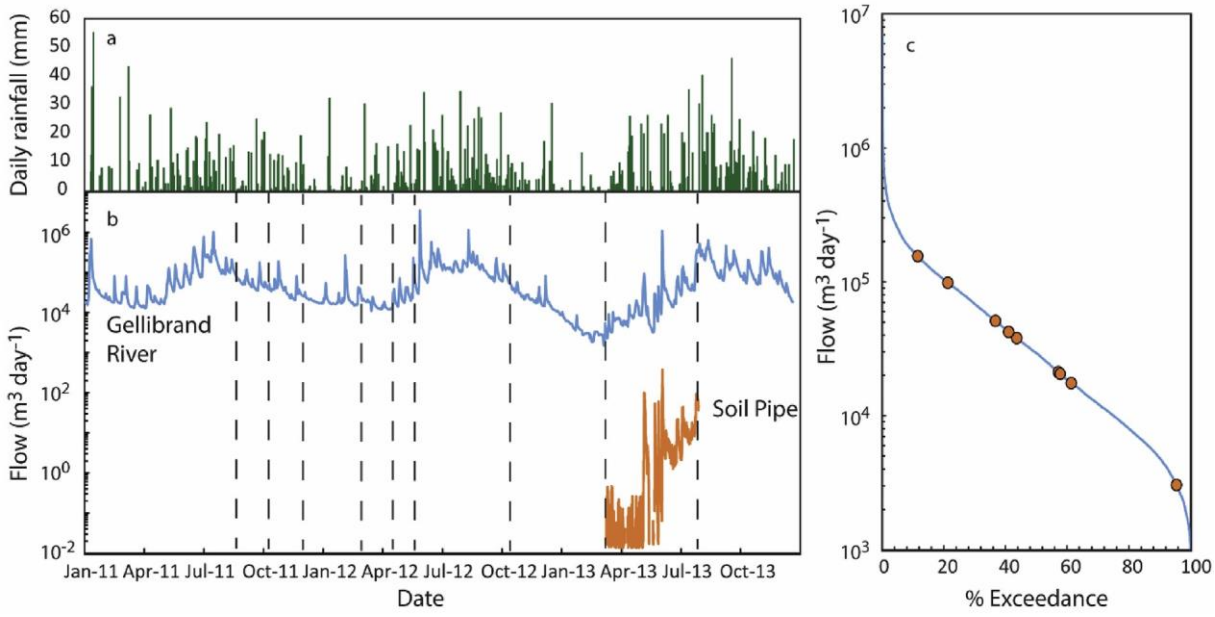

Fig. 2. a. Daily rainfall at Forrest (Bureau of Meteorology, 2018). 2b. Streamflow in the Upper Gellibrand River at gauge 235202 (Fig. 1) and flow from the soil pipe. Dashed lines show timing of geochemical sampling. 2c. Flow frequency curve showing the percentage of time that streamflows between 1990 and 2017 at gauge 235202 were exceeded. Symbols show timing of geochemical sampling. Streamflow data from Department of Land, Water, Environment and Planning (2018).

Meyer-Olkin measure of sample adequacy is 0.54 and applying the Bartlett sphericity test produces a chi-squared statistic for 21 degrees of freedom of 419 with a significance of < 0.001. This indicates that variables are not orthogonal, but are correlated. A varimax rotation was used to reduce the overlap of the original variables.

3.4. Estimating mean transit times

Mean transit times (τ_m) were estimated using lumped parameter models implemented in an updated version (TracerLPM V2) of the TracerLPM Excel workbook (Jurgens et al., 2012) that includes the gamma model (Amin and Campana, 1996). The ^3H activity of water sampled at time t ($C_o(t)$) is related to the input of ^3H (C_i) over time via the convolution integral:

$$C\,t_o(\,) = \int_0^{\infty} C\,t_i(-\tau\,g\,\tau\,e)\,(\,)^{-\lambda\tau} d\tau \qquad (1)$$

(Maloszewski and Zuber, 1982; Maloszewski, 2000) where τ is the transit time, t-τ is the time when water entered the catchment, λ is the decay constant (0.0563 yr^{-1} for ^3H), and g(τ) is the response function that describes the distribution of flow paths and ages in the flow system. The annual average ^3H activities of rainfall in Melbourne (Tadros et al., 2014; International Atomic Energy Agency, 2017) were used as the ^3H input function. ^3H activities of rainfall in Melbourne peaked at approximately 62 TU in 1965 and then declined exponentially. The average annual ^3H activities of present-day rainfall in this area are approximately 2.8 TU (Tadros et al., 2014; Cartwright and Morgenstern, 2015, 2016a; Howcroft et al., 2018; Hofmann et al., 2018). A ^3H activity of 2.8 TU was also used for rainfall from the years before the atmospheric nuclear tests.

Several lumped parameter models were considered. The exponential flow model applies to homogeneous unconfined aquifers of constant thickness with uniform recharge where water from the entire aquifer is sampled via a fully penetrating well or stream. The exponential-piston flow model describes flow in unconfined aquifers with regions of vertical recharge through the unsaturated zone (piston flow) above a groundwater flow system with an exponential age distribution. TracerLPM uses the EPM ratio to specify the relative importance of piston and exponential flow. For an EPM ratio of 0, the model is equivalent to the exponential flow model, whereas EPM ratios of >5 produces a model that is close to piston flow. The dispersion model is derived from the one-dimensional advection-dispersion transport equation. This model requires a dispersion parameter (DP), which describes the relative importance of dispersion relative to advection, to be defined (DP is the inverse of the more commonly reported Peclet number). These lumped parameter models have reproduced the time series of tracer concentrations (including ^{3}H) in similar scale flow systems elsewhere (e.g., Maloszewski and Zuber, 1982; Maloszewski, 2000; Zuber et al., 2005; Blavoux et al., 2013; Gusyev et al., 2013; Morgenstern et al., 2015). The gamma model (Amin and Campana, 1996; Kirchner et al., 2000; Hrachowitz et al., 2010a) has two parameters: α describes the transit time distribution; and β is a scaling parameter ($\tau_m = \alpha\beta$). At $\alpha = 1$, the gamma model becomes the exponential model and at $\alpha > 1$ it reproduces the long tails of tracers that are commonly observed in flow systems.

Response functions for these lumped parameter models are summarised by Maloszewski and Zuber (1982), Amin and Campana (1996), Zuber et al. (2005), Kirchner et al. (2000), Hrachowitz et al. (2010a), and Jurgens et al. (2012). Mean transit times were calculated by matching the measured ^{3}H activity in the sample with that predicted from the lumped parameter model. Mean transit times are related to the volume of the water store (V) that generates the discharge from the catchment (Q) via

$$V = Q\,\tau_m \quad (2)$$

(Maloszewski and Zuber, 1982; Morgenstern et al., 2010; Gusyev et al., 2016).

4. Results

4.1. Streamflow and pipe flow

Both the streamflow and the volume of water discharging from the soil pipes were seasonably variable. Higher streamflows resulting from a combination of higher rainfall (Fig. 2a) and lower evapotranspiration rates occurred in the austral winter months (Fig. 2b). During the sampling period between January 2011 and December 2013, streamflows in the upper Gellibrand River at gauge 235202 ranged between 1.5×10^3 and 3.5×10^6 m^3/day (Fig. 2b). The samples were collected at streamflows representing the 12th to 95th percentiles of streamflows between 1990 and 2017 (Fig. 2c). The daily discharge from soil pipe SP1 between March 2013

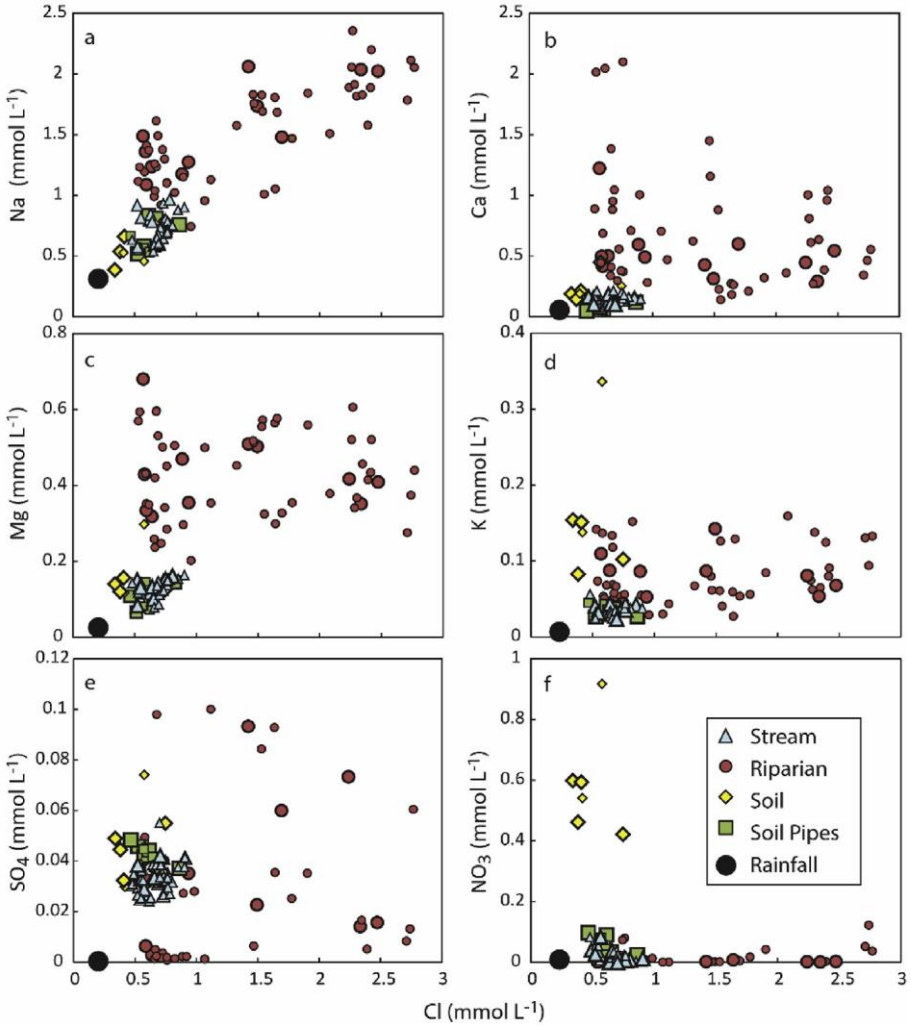

Fig. 3. Molar concentrations of Na (3a), Ca (3b), Mg (3c), K (3d), SO_4 (3e) and NO_3 (3f) vs. Cl in the water from the stream, riparian zone, soils, and soil pipes in the upper Gellibrand catchment (data from Table S1, larger symbols denote samples collected in the higher rainfall spring and winter months). Rainfall data from Blackburn and McLeod (1983), Cartwright and Morgenstern (2015), Cartwright et al. (2018), and Howcroft et al. (2018).

and August 2013 pipe was between 1 and 400 m^3/day (although the highest values exceed the calibration curve) and the temporal variation in discharge was similar to streamflow (Fig. 2b). The net discharge from SP1 of ~5600 m^3 over this period was ~0.1% of the streamflow recorded at gauge 23502.

4.2. Major ion geochemistry

The concentrations of all of the major ions in the water from the streams, soils, riparian zones, and soil pipes are elevated relative to those of typical rainfall in southeast Australia (Fig. 3). Na is the major cation (30–80% on a molar basis) in all of the waters, followed by Ca (5–56%), Mg (8–23%), and K (1–22%). Cl and HCO_3 are the major anions (17–86% and 13–82% on a molar basis, respectively) with minor NO_3 and SO_4 (both < 1%). The geochemistry of the different waters is mutually different (Table S1, Fig. 3). Relative to the stream water, the water from the riparian zone has higher concentrations of most major ions except for NO_3, although SO_4 concentrations are highly variable. For example, the mean and median concentrations of Cl in the riparian zone waters are 48.8 ± 26.3 and 47.1 mg/L, respectively, whereas the stream waters have a mean Cl concentration of 23.5 ± 3.7 mg/L and a median Cl concentration of 24.0 mg/L (Table 1). The soil water has higher NO_3 (mean = 19.2 ± 7.0, median =18.6 mg/L) and K (mean = 5.87 ± 2.86, median = 5.65 mg/L) concentrations than the stream waters (mean and median NO_3 concentrations =1.25 ± 1.22 and 0.92 mg/L; mean and median K concentrations = 1.38 ± 0.25 and 1.34 mg/L). By contrast, the stream water and the water from the soil pipes have similar concentrations of major ions. Despite being collected at a range of flow conditions, there is no systematic seasonal variation in the geochemistry of the waters, including that from the streams (Fig. 3). As is the case throughout southeast Australia, the increase in Cl concentrations in soil water or

groundwater in southeast Australia over those in rainfall is primarily due to evapotranspiration, whereas a combination of evapotranspiration and mineral dissolution increase cation and Si concentrations (e.g., Herczeg et al., 2001; Tweed et al., 2005; Cartwright and Morgenstern, 2015, 2018; Cartwright et al., 2018). The high NO_3 concentrations in the soils probably reflect decomposition and dissolution of organic matter.

PCA was used to assess the similarity of the water geochemistry (Fig. 4). The largest three principle components, PC1, PC2, and PC3 explain 42.0%, 23.2%, and 14.8% of the total variance, respectively (cumulatively 80.0% of the variance). The PCA confirms that the geochemistry of water from the soil pipes is most closely similar to that of the streams and distinctly different to the soil and riparian zone waters.

Table 1
Summary of water chemistry from upper Gellibrand catchment.

	Stream	Riparian	Soil Pipes	Soils
Cl mg/L	17.0–32.2[a]	11.3–98.1	16.5–32.3	9.2–32.7
	23.52 ± 3.73	48.82 ± 26.33	24.13 ± 6.48	19.17 ± 6.99
	23.99	47.07	21.98	18.64
NO_3 mg/L	0.02–5.16	0.001–8.09	0.05–6.03	bd-75.8
	1.25 ± 1.22	0.86 ± 1.59	2.60 ± 2.11	19.17 ± 6.99
	0.92	0.18	1.67	18.64
SO_4 mg/L	2.33–5.29	0.09–34.8	2.84–9.59	2.12–7.12
	3.27 ± 0.52	3.44 ± 5.05	4.38 ± 1.56	4.10 ± 1.57
	3.22	1.60	4.26	3.80
Na mg/L	12.4–22.2	14.8–54.2	11.9–19.2	8.89–25.6
	16.32 ± 2.94	34.24 ± 9.62	15.14 ± 2.61	16.68 ± 6.07
	15.66	34.02	14.33	15.66
K mg/L	0.92–2.20	1.06–6.23	1.03–1.76	2.90–13.2
	1.38 ± 0.25	3.07 ± 1.40	1.30 ± 0.28	5.87 ± 2.86
	1.34	2.65	1.22	5.65
Ca mg/L	3.70–8.61	4.51–84.2	1.58–5.16	5.81–18.1
	5.74 ± 1.38	26.45 ± 18.33	3.35 ± 1.42	10.35 ± 3.53
	5.71	20.10	3.65	9.75
Mg mg/L	1.92–3.97	2.97–16.5	1.47–3.70	2.85–7.23
	3.13 ± 0.59	10.34 ± 2.89	2.61 ± 0.81	4.21 ± 1.42
	3.25	10.44	2.68	3.64
$\delta_{18}O$ ‰ SMOW	−5.8–−4.5 −5.16 ± 0.33	−5.8–−4.3 −5.09 ± 0.29	−5.7–−5.1 −5.40 ± 0.22	−6.8–−2.4 −4.87 ± 1.11
	−5.18	−5.09	−5.40	−4.95
δ_2H ‰ SMOW	−32–−25	−30–25	−33–−27	−39.1–−9.8
	−27.2 ± 1.7	−28.0 ± 1.1	−30.1 ± 1.9	−28.1 ± 8.0
	−26.7	−28.1	−30.1	−30.3
^3H TU	1.84–2.06	1.35–2.39	1.80–2.25	2.22

[a] Data listed as Range, Average and Standard Deviation, Median. Data is from Table S1.

A comparison of PC values using T-tests assuming unequal variances confirms that the PC1 values of the riparian zone waters are significantly different ($p < 0.05$) to those of the other waters. Likewise, the PC3 values of the soil water are significantly different to those of the other waters.

4.3. Stable isotopes

The $\delta^{18}O$ and δ^2H values of the waters lie close to the Melbourne and global meteoric water lines (Fig. 5). The mean, median and ranges of $\delta^{18}O$ and δ^2H values of the water from the riparian zone, soils, and soil pipes are mutually similar (Table 1, Fig. 5). Overall, the of $\delta^{18}O$ and δ^2H values of water from these stores are slightly lower than those of average rainfall in Melbourne, which is ~160 km east of the study area ($\delta^{18}O$ =−5.03‰, δ^2H =−28.4‰: Hollins et al., 2018). This observation may indicate preferential retention of water sourced from winter rains with lower $\delta^{18}O$ and δ^2H values in the catchment, although it may also reflect the regional variability of the $\delta^{18}O$ and δ^2H values rainfall. The $\delta^{18}O$ and δ^2H values of the soil waters define a much broader range of $\delta^{18}O$ and δ^2H values than those of the other water stores (Table 1). The $\delta^{18}O$ and δ^2H values of the soil waters from different depths at individual sites may vary by several per mil. Generally, the

shallowest samples (from ~20 cm depth) have higher $\delta^{18}O$ and $\delta^{2}H$ values, which probably result from evaporation from the shallow soils. If evaporation occurs at relatively high humidity in the soil, the slopes of local evaporation lines may be similar to that of the meteoric water line (Clark and Fritz, 1997).

4.4. Tritium activities

The expected ^{3}H activities of present-day average annual rainfall in this region of southeast Australia interpolated from the data of Tadros et al. (2014) are 2.6–3.0 TU. In agreement with that prediction, a 12 month rainfall sample from Yarra Junction (180 km east of the study area) collected in August 2015 has a ^{3}H activity of 2.76 TU and a 9 month sample from southeast Melbourne (160 km east of the study area) collected in July 2013 has a ^{3}H activity of 2.72 TU (Atkinson, 2014; Cartwright et al., 2018). The ^{3}H activities of the waters from the streams, soils, riparian zone, and soil pipes overlap (Table 2) and are lower than those of rainfall. The ^{3}H activities of the stream water range from 1.80 to 2.06 TU with little difference between those in the Barramunga and upper Gellibrand Rivers. The ^{3}H activities of stream water at B1 and UG4 were slightly lower during the March low flows than at other times (Table 2). This is a trend observed in other headwater streams in southeast Australia (Cartwright and Morgenstern, 2015, 2016a; 2016b; Howcroft et al., 2018; Hofmann et al., 2018; Cartwright et al., 2018) that probably reflects the mobilisation of shallower water stores following winter rainfall. However, the seasonal differences in the ^{3}H activities in the upper Gellibrand streams (~0.25 TU) are much smaller than in those other catchments. The ^{3}H activities of water from the soil pipes range between 1.80 and 2.25 TU, whereas ^{3}H activities of the riparian zone waters are more variable (1.35–2.39 TU). One sample of soil water has a ^{3}H activity of 2.22 TU.

5. Discussion

The combined geochemical data allows the origins and transit times of the waters that generate the streamflow in the upper Gellibrand catchment to be determined.

5.1. Mean transit times

The ^{3}H data set (Table 2) is relatively small (n =22) and waters are from flow systems with potentially different flow geometries (riparian groundwater, the streams, the soil water, and the soil pipes). This presents difficulties in estimating mean transit times. For example, the exponential-piston flow model plausibly represents the geometry of groundwater flow (vertical recharge through the unsaturated zone and flow with an exponential age distribution within the saturated zone), while near vertical flow in the soils may be better described using the

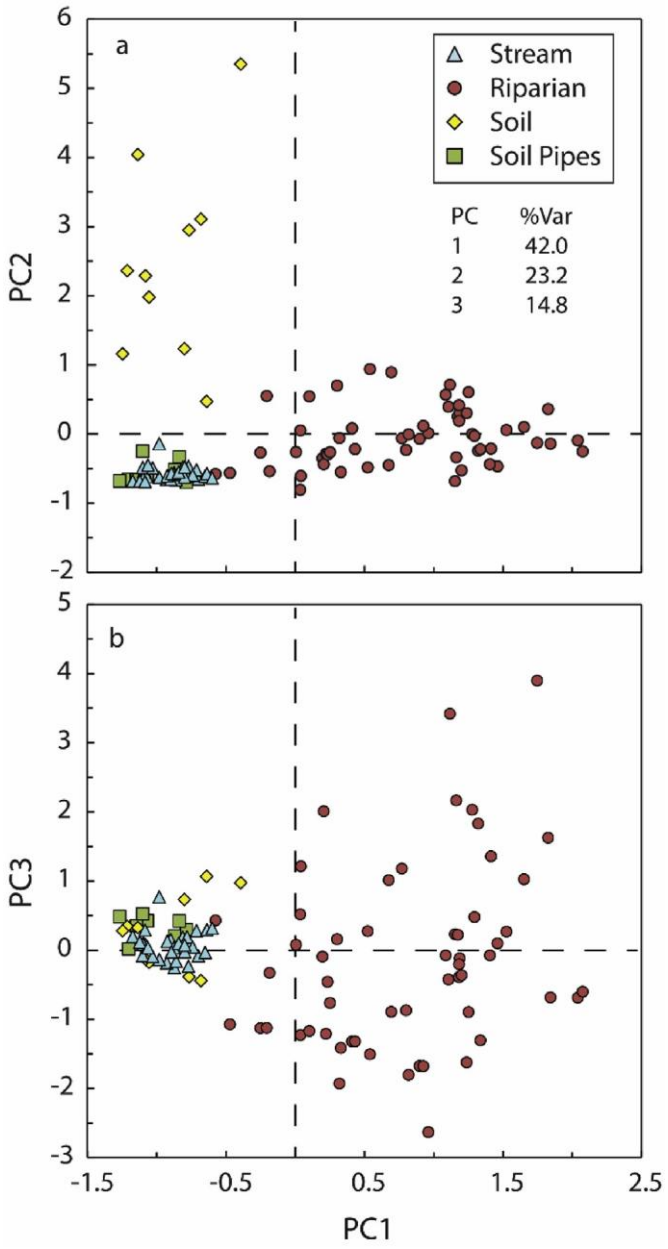

Fig. 4. Principle component analysis using the major ion concentrations. 4a. PC1 vs. PC2. 4b. PC1 vs. PC3. %Var is the percentage variance explained by the three principle components (PC). Based on this analysis, the geochemistry of stream waters is most similar to that of the soil pipes.

dispersion model. In recognition of these difficulties, mean transit times were estimated using the exponential, exponential-piston flow, dispersion and gamma models. For the exponential-piston flow model, the EPM ratios were 0.33 (25% piston flow, 75% exponential flow) and 1 (50% piston flow, 50% exponential flow). For the dispersion model, a DP value of 0.1, which is appropriate for tens to hundreds of metres scale flow systems, was used (Maloszewski, 2000). The gamma model had a α value of 3.

The mean transit times of all the waters range between 3 and 57 years (Fig. 6, Table 2). The mean transit times of the Barramunga and Gellibrand Rivers overlap and are between 11 and 26 years. At two sites (B1 and UG4) the mean transit times at the lowest flows (March) are slightly longer than those at other times; however as noted above, the differences are small. The mean transit times of the riparian waters are between 3 and 57 years (i.e. these waters have both the shortest and

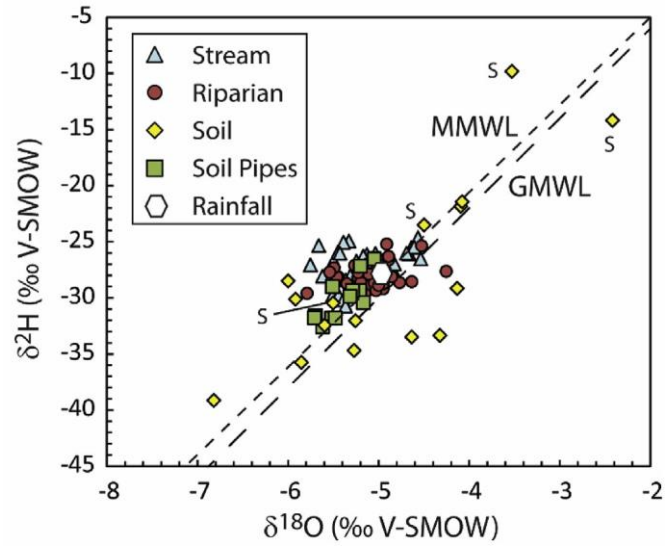

Fig. 5. $\delta^{18}O$ and $\delta^{2}H$ values of waters from the upper Gellibrand catchment (data from Table S1). MMWL and GMWL are the Melbourne and Global Meteoric Water Lines (Hollins et al., 2018). S denotes the shallowest soil water samples (~20 cm depth). Rainfall is the weighted average of Melbourne rain (Hollins et al., 2018).

Table 2 ^{3}H activities and calculated mean transit times in the upper Gellibrand catchment.

Site[a]	Date	^{3}H (TU)	Mean Transit Time (yr)[b]				
			EMM	Gamma (3)	DM (0.1)	EPM (0.33)	EPM (1)
Rivers							
B1	Mar-12	2.06	13.8	10.5	10.7	11.2	11.1
B1	Oct-12	1.95	19.0	12.5	12.9	15.6	13.2
B2	Mar-12	1.84	24.1	17.6	15.4	21.2	16.2
B2	Apr-12	2.01	16.2	11.6	11.7	13.0	12.0
B2	Oct-12	1.90	21.3	14.7	13.9	18.2	14.4
B2	Aug-13	2.04	14.8	10.9	11.1	11.8	11.5
UG4	Mar-12	1.80	26.0	21.1	18.6	23.0	17.9
UG4	Apr-12	1.90	21.3	14.7	13.9	18.2	14.4
UG4	Oct-12	1.87	22.7	16.0	14.6	19.9	15.3
Riparian Zone							
B1-2[c]	Oct-12	1.94	19.4	13.4	13.1	16.1	13.5
B1-3	Oct-12	1.60	36.1	37.0	42.6	32.7	30.7
B2-1	Apr-12	1.61	35.6	36.6	42.0	32.2	29.6
B2-2	Apr-12	1.35	51.2	48.1	53.2	45.9	56.7
UG2-1	Oct-12	1.85	23.6	17.0	15.1	20.8	15.9
UG3-1	Apr-12	2.32	5.8	5.2	5.0	5.1	4.5
UG3-2	Apr-12	2.39	4.5	3.7	3.3	3.9	3.3
Soil							
UG3-M[d]	Oct-12	2.22	8.2	7.2	7.6	7.1	7.0
Soil Pipes							
SP1	Oct-12	2.09	12.6	9.9	10.1	10.2	10.7
SP1	Aug-13	2.19	9.1	7.8	8.3	7.7	8.0
SP2	Oct-12	1.80	26.0	21.1	18.6	23.0	17.9
SP3	Oct-12	2.03	15.2	11.1	11.3	12.2	11.7
SP3	Aug-13	2.25	6.7	6.6	6.9	6.4	6.2

[a] Sample sites are on Fig. 1. Soil pipes are in the Barramunga catchment between B1 and B2.

[b] Lumped parameter models: D = Dispersion; EMM =exponential; EXP = exponential-piston flow (α, DP, and EPM values in brackets).

[c] Piezometer number at site. [d] Sample from ~50 cm depth.

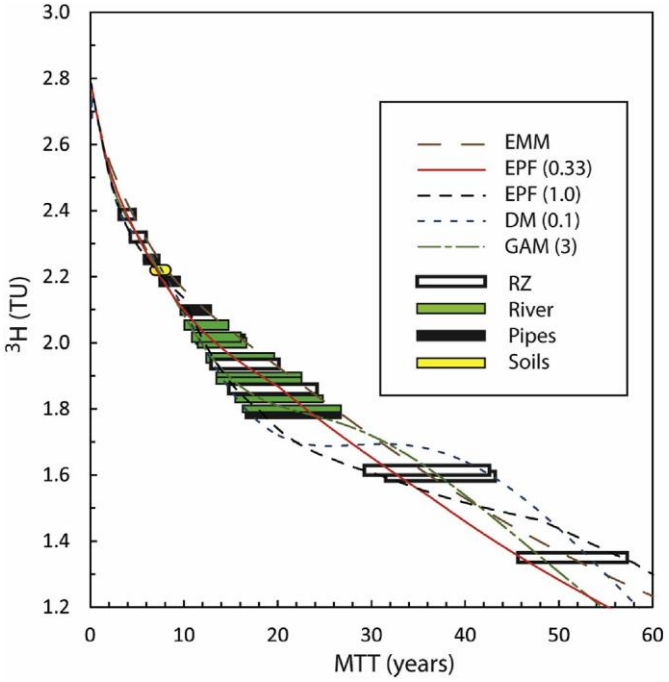

Fig. 6. Summary of Mean Transit Times (MTT) calculated using the Exponential (EMM), Exponential-Piston Flow (EPF), Dispersion (DM), and Gamma (GAM) lumped parameter models (values of EPM, DP, and α variables in brackets). RZ is the riparian zone water and the ^{3}H activities are in Table S1.

longest mean transit times) and differ between sites. Riparian water from B2 has the longest mean transit times (30–57 years), while that from UG3 is significantly younger (mean transit times of 3–6 years). Water from the soil pipes has mean transit times of between 6 and 26 years, while the single sample of soil water has a mean transit time of 7–8 years. The long mean transit times are consistent with the conclusions made from the major ion and stable isotope geochemistry that dissolution of organic matter, mineral dissolution, and evapotranspiration have occurred as these processes occur over timescales of several years.

The volume of the stores of water that generates streamflow may be estimated from Eq. (2). Assuming that all the streamflow draining through gauge 235202 has a mean transit time of 12 years (average of the minimum and maximum mean transit times in Table 2), the average annual streamflow of 2.3×10^7 m^3 implies a storage volume of $\sim 2.8 \times 10^8$ m^3. If much of this water flows through the catchments via the soil pipes, the volume of water feeding those pipes is considerable.

5.2. Uncertainties in mean transit times

Where ^{3}H activities exceed 2 TU, the mean transit times calculated from the different lumped parameter models are similar. For example, at a ^{3}H activity of 2.25, the mean transit time from the suite of models varies between 6 and 7 years. However, for lower ^{3}H activities there is a greater difference in the estimated mean transit times between the different models. For example, at a ^{3}H activity of 1.6, the range of mean transit times from the different models varies between 31 and 43 years.

The ^{3}H activities of modern rainfall in this area are 2.8 ± 0.2 TU, which represents a relative uncertainty of ±7% (Tadros et al., 2014). This uncertainty has most influence on mean transit times of the waters with high ^{3}H activities. This may be illustrated using the exponentialpiston flow model with an EPM ratio of 1; closely similar results are observed for the other models. For the water with the highest ^{3}H activity (2.4 TU), allowing the ^{3}H activities of modern rainfall to vary between 2.6 and 3.0 TU produces mean transit times of between 1.5 and 6.8 years (a relative uncertainty of ±21%). By contrast, for a water with a ^{3}H activity of 1.5 TU, the variation in mean transit times is < 0.1 years. Uncertainties in the ^{3}H activity of past rainfall exert a greater influence on the mean transit times of the low ^{3}H samples. If the ^{3}H activities of past rainfall are varied by a similar relative amount (±7%), the range of mean transit times for a water with ^{3}H activity of 1.5 TU is 35.5–48.4 years, which is a relative uncertainty of ±16%.

Propagating the larger of the analytical uncertainties (± 5%) results in an overall uncertainty of ± 1.5 years at a ^{3}H activity of 2 TU and ± 2.2 years at a ^{3}H activity of 1.5 TU. The mean transit times were calculated using the ^{3}H activities of average annual rainfall. The high rainfall in the upper Gellibrand area probably results in recharge occurring throughout the year. However, some summer rainfall may be lost by evapotranspiration and thus the ^{3}H activities of the water that recharges the catchment may be different to that of average rainfall (Morgenstern et al., 2010; Blavoux et al., 2013). The observation that the δ^{18}O and δ^2H values of the water stores in the upper Gellibrand catchment are slightly lower than those of average rainfall may be due to preferential winter recharge. However, because the ^{3}H activities in summer rainfall in southeast Australia are close to the average annual ^{3}H activities (Cartwright and Morgenstern, 2015, 2016a; Cartwright et al., 2018), the uncertainties resulting from using the average annual ^{3}H activity are considered to be minor (Morgenstern et al., 2010).

Aggregation, or the macroscopic mixing of water with different mean transit times (e.g., where multiple flow systems discharge into a stream), results in mean transit times being underestimated (Kirchner, 2016; Stewart et al., 2017). The uncertainty due to aggregation is difficult to assess. Cartwright and Morgenstern (2016a) and Howcroft et al. (2018) estimated that, for waters with the range of mean transit times similar to those in this study, it may be as high as ±15%. The uncertainties in mean transit times caused by hydrodynamic dispersion in aquifers with heterogeneous hydraulic conductivities are probably of similar magnitude

(Cartwright et al., 2018). The effect of aggregation is higher if waters with widely different mean transit times mix (Stewart et al., 2017). It will therefore probably mainly affect water with longer transit times if mixing with recently recharged waters occurs.

These uncertainties hamper a precise determination of mean transit times. Assuming that the uncertainties are uncorrelated and have Gaussian distributions, the net uncertainty is the square root of the sum of the squares of the individual uncertainties. For the waters with lower ^{3}H activities, the uncertainties in mean transit times due to choice of the lumped parameter model, aggregation or mixing, and errors in the assumed ^{3}H input are each approximately ±15%, while the analytical error is up to ±5%. This implies an overall relative uncertainty of approximately ± 25%. For high ^{3}H waters, the impact of the uncertainties in the ^{3}H activity of modern rainfall is higher, but the errors resulting from having to choose a lumped parameter model and aggregation are lower, which results in a similar overall uncertainty.

5.3. Conceptual model

The mean transit times of all of the water stores in the upper Gellibrand catchment at a wide range of flow conditions are years to decades, which in turn implies that there are significant of water stores in this upper catchment that sustains streamflow. The relatively long mean transit times implies that the direct input of recent rainfall is less important than older water displaced from the catchment. Thus, this catchment is a clear example of celerity being significantly shorter than the transit times.

The major ion geochemistry of the stream water in the upper Gellibrand catchment most closely represents that of the soil pipes (Figs. 3 and 4), and the water discharging from the pipes likely contributes much of the streamflow in this upper catchment (Fig. 7). Many of the soil pipes are perennial and can thus contribute to streamflow throughout the year. While the distribution and frequency of soil pipes is not well known they are common features in the upper catchment, particularly in the Barramunga subcatchment. In common with the streamflow, the discharge from the soil pipes increases following periods of high rainfall (Fig. 2). The calculated mean transit times imply that the soil pipe water is stored for several years within the catchment before discharge. This in turn suggests that the increase in discharge is not the simple transmission of recent rainfall through the macropores. The water in the soil pipes may be mainly derived from a relatively large store in the more weathered parts of the regolith. The observation that the mean transit times are lower in winter suggests that younger stores of water are mobilised via the soil pipes at those times (perhaps via the ephemeral pipes that flow during the wetter periods).

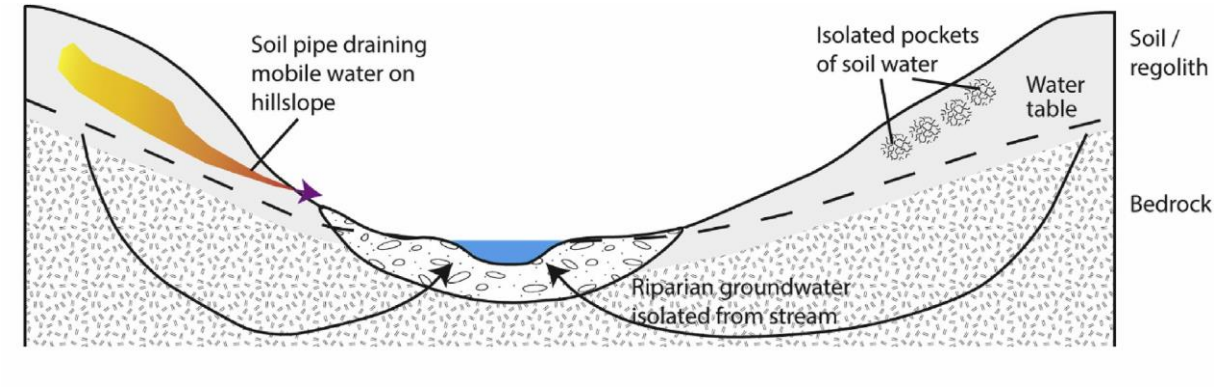

Fig. 7. Schematic model of the upper Gellibrand catchment. Some soil water is isolated on the hillslopes and the mobile water from the unsaturated zone drains through the soil pipes. The groundwater in the riparian zone is not well connected to the stream, possibly due to clay-rich streambed sediments.

The riparian zone waters have the most distinct major ion geochemistry and the longest transit times. Given that these waters occur adjacent to gaining streams, it is surprising that this pool of water does not contribute significantly to streamflow. While the hydraulic properties of the stream sediments are not well constrained, the streambed commonly consists of fine-grained organic-rich sediment that may restrict the inflows of this water. Alternatively, compartmentalisation of the shallow groundwater due to the presence of clays in the weathered rocks may occur.

The ^{3}H activity and hence the estimated transit time of the soil water is similar to that of the other waters in the catchment. While this is based on a single sample and thus it is not clear how representative the estimate is, the major ion geochemistry of the soil water in general requires that it has been present in the catchment for sufficient time for evapotranspiration and mineral dissolution to occur. Based on the geochemistry, the soil waters represent a different reservoir to the water sampled from the soil pipes. The soil water sampled from the lysimeters is likely to be relatively mobile, and it is not clear why this water does not drain via the soil pipes. Possibly the water in the soils is compartmentalised on scales of metres to tens-of-metres (e.g., Evaristo et al., 2015) due to the occurrence of clay layers such that hillslopescale movement is inhibited.

6. Conclusions

This study illustrates how geochemistry allows an assessment of both the sources of water in a headwater catchment that contribute to streamflow and the timescales of water movement. Compared with stream water or groundwater, estimates of mean transit times of soil waters and water mobilised via macropores are rare; however, determining these is important for a holistic understanding of catchment behaviour. There are several distinct stores of water in the upper Gellibrand catchment, and flow through macropore (soil pipes) is important in generating the streamflow. Given that the streams are gaining, the small contribution of groundwater from the riparian zone immediately adjacent to the stream is surprising but may relate to the nature of the streambed sediments. The long mean transit times implies that these upper catchments will be resilient to year-on-year variations in rainfall but will potentially be affected by decadal scale climate change. Landuse change such as deforestation also changes long-term recharge rates and may similarly affect the catchment water balance.

As with many other catchments in southeast Australia, the mean transit times of the stream water in the upper Gellibrand catchment are years to decades and significantly longer than those recorded in headwater catchments elsewhere (McGuire and McDonnell, 2006; Stewart et al., 2010). The long mean transit times

possibly reflect clay-rich low hydraulic conductivity soils, deeply weathered regolith with high volumes of water in storage, and/or the high evapotranspiration rates of the eucalypt vegetation.

Acknowledgements

Funding for this project was provided by Monash University and the National Centre for Groundwater Research and Training. The National Centre for Groundwater Research and Training was an Australian Government initiative supported by the Australian Research Council and the National Water Commission via Special Research Initiative SR0800001. We thank Massimo Raveggi and Rachelle Pearson for assistance with the geochemical analyses and Bryant Jurgens for making available the updated TracerLPM package.

Appendix A. Supplementary data

Supplementary data to this article can be found online at https:// doi.org/10.1016/j.apgeochem.2018.10.018.

References

Alexander, R.B., Boyer, E.W., Smith, R.A., Schwarz, G.E., Moore, R.B., 2007. The role of headwater streams in downstream water quality. J. Am. Water Resour. Assoc. 43, 41–59. https://doi.org/10.1111/j.1752-1688.2007.00005.x.

Amin, I.E., Campana, M.E., 1996. A general lumped parameter model for the interpretation of tracer data and transit time calculation in hydrologic systems. J. Hydrol. 179, 1–21. https://doi.org/10.1016/0022-1694(95)02880-3.

Anderson, A., Weiler, M., Alila, Y., Hudson, R., 2009. Subsurface flow velocities in a hillslope with lateral preferential flow. Water Resour. Res. 45, W11407. https://doi. org/10.1029/2008WR007121.

Atkinson, A.P., 2014. Surface Water-groundwater Interactions in an Upland Catchment (Gellibrand River, Otways Ranges, Victoria, Australia). PhD Thesis. Monash University.

Atkinson, A., Cartwright, I., Gilfedder, B., Hofmann, H., Unland, N., Cendón, D., Chisari, R., 2015. A multi-tracer approach to quantifying groundwater inflows to an upland river; assessing the influence of variable groundwater chemistry. Hydrol. Process. 29, 1–12. https://doi.org/10.1002/hyp.10122.

Atkinson, A.P., Cartwright, I., Gilfedder, B.S., Cendón, D.I., Unland, N.P., Hofmann, H., 2014. Using ^{14}C and ^{3}H to understand groundwater flow and recharge in an aquifer window. Hydrol. Earth Syst. Sci. 18, 4951–4964. https://doi.org/10.5194/hess-184951-2014.

Australian Soil Resource Information System, 2018. www.asris.csiro.au/index.html.

Blackburn, G., McLeod, S., 1983. Salinity of atmospheric precipitation in the Murray Darling drainage division, Australia. Aust. J. Soil Res. 21, 400–434. https://doi.org/ 10.1071/SR9830411.

Blavoux, B., Lachassagne, P., Henriot, A., Ladouche, B., Marc, V., Beley, J.-J., Nicoud, G., Olive, P., 2013. A fifty-year chronicle of tritium data for characterising the functioning of the Evian and Thonon (France) glacial aquifers. J. Hydrol. 494, 116–133. https://doi.org/10.1016/j.jhydrol.2013.04.029.

Botter, G., Bertuzzo, E., Rinaldo, A., 2010. Transport in the hydrologic response: travel time distributions, soil moisture dynamics, and the old water paradox. Water Resour. Res. 46, W03514. https://doi.org/10.1029/2009WR008371.

Boucher, S., Powell, J., 1994. Gullying and tunnel erosion in Victoria. Geogr. Res. 32, 17–26. https://doi.org/10.1111/j.1467-8470.1994.tb00657.x.

Bureau of Meteorology, 2018. Commonwealth of Australia Bureau of Meteorology. www. bom.gov.au.

Cartwright, I., Irvine, D., Burton, C., Morgenstern, U., 2018. Assessing the controls and uncertainties on mean transit times in contrasting headwater catchments. J. Hydrol. 557, 16–29. https://doi.org/10.1016/j.jhydrol.2017.12.007.

Cartwright, I., Morgenstern, U., 2015. Transit times from rainfall to baseflow in headwater catchments estimated using tritium: the Ovens River, Australia. Hydrol. Earth Syst. Sci. 19, 3771–3785. https://doi.org/10.5194/hess-19-3771-2015.

Cartwright, I., Morgenstern, U., 2016a. Contrasting transit times of water from peatlands and eucalypt forests in the Australian Alps determined by tritium: implications for vulnerability and the source of water in upland catchments. Hydrol. Earth Syst. Sci. 20, 4757–4773. https://doi.org/10.5194/hess-20-4757-2016.

Cartwright, I., Morgenstern, U., 2016b. Using tritium to document the mean transit time and sources of water contributing to a chain-of-ponds river system: implications for resource protection. Appl. Geochem. 75, 9–19. https://doi.org/10.1016/j. apgeochem.2016.10.007.

Cartwright, I., Morgenstern, U., 2018. Using tritium and other geochemical tracers to address the "old water paradox" in headwater catchments. J. Hydrol. 563, 13–21. https://doi.org/10.1016/j.jhydrol.2018.05.060.

Clark, I.D., Fritz, P., 1997. Environmental Isotopes in Hydrogeology. CRC press.

Coplen, T.B., 1988. Normalization of oxygen and hydrogen isotope data. Chem. Geol. 72, 293–297. https://doi.org/10.1016/0168-9622(88)90042-5.

Crouch, R., McGarity, J., Storrier, R., 1986. Tunnel formation processes in the Riverina area of NSW, Australia. Earth Surf. Process. Landforms 11, 157–168. https://doi.org/ 10.1002/esp.3290110206.

Department of Environment Land Water and Planning, 2018. State Government Victoria Department of Environment Environment, Land, Water and Planning Water Measurement Information System. http://data.water.vic.gov.au/monitoring.htm.

Duvert, C., Stewart, M.K., Cendón, D.I., Raiber, M., 2016. Time series of tritium, stable isotopes and chloride reveal short-term variations in groundwater contribution to a stream. Hydrol. Earth Syst. Sci. 20, 257–277. https://doi.org/10.5194/hess-20-2572016.

Edmunds, W.M., 2009. Geochemistry's vital contribution to solving water resource problems. Appl. Geochem. 24, 1058–1073. https://doi.org/10.1016/j.apgeochem.2009. 02.021.

Evaristo, J., Jasechko, S., McDonnell, J.J., 2015. Global separation of plant transpiration from groundwater and streamflow. Nature 525, 91–94. https://doi.org/10.1038/ nature14983.

Freeman, M.C., Pringle, C.M., Jackson, C.R., 2007. Hydrologic connectivity and the contribution of stream headwaters to ecological integrity at regional scales. J. Am. Water Resour. Assoc. 43, 5–14. https://doi.org/10.1111/j.1752-1688.2007.00002.x.

Furuichi, K., Katayama, K., Date, H., Takeishi, T., Fukada, S., 2016. Tritium sorption behavior on the percolation of tritiated water into a soil packed bed. Fusion Eng. Des. 109–111, 1371–1375. https://doi.org/10.1016/j.fusengdes.2015.12.019.

Gusyev, M.A., Morgenstern, U., Stewart, M.K., Yamazaki, Y., Kashiwaya, K., Nishihara, T., Kuribayashi, D., Sawano, H., Iwami, Y., 2016. Application of tritium in precipitation and baseflow in Japan: a case study of groundwater transit times and storage in Hokkaido watersheds. Hydrol. Earth Syst. Sci. 20, 1–16. https://doi.org/10.5194/ hess-20-1-2016.

Gusyev, M.A., Toews, M., Morgenstern, U., Stewart, M., White, P., Daughney, C., Hadfield, J., 2013. Calibration of a transient transport model to tritium data in streams and simulation of groundwater ages in the western Lake Taupo catchment, New Zealand. Hydrol. Earth Syst. Sci. 17, 1217–1227. https://doi.org/10.5194/hess17-1217-2013.

Herczeg, A.L., Dogramaci, S.S., Leaney, F.W., 2001. Origin of dissolved salts in a large, semi-arid groundwater system: Murray Basin, Australia. Mar. Freshw. Resourc. 52, 41–52. https://doi.org/10.1071/MF00040.

Herczeg, A.L., Edmunds, W.M., 2000. Inorganic ions as tracers. In: Cook, P., Herczeg, A. (Eds.), Environmental Tracers in Subsurface Hydrology. Kluwer Academic Publishers, Boston.

Hofmann, H., Cartwright, I., Morgenstern, U., 2018. Estimating retention potential of headwater catchment using Tritium time series. J. Hydrol. 561, 557–572. https://doi.org/10.1016/j.jhydrol.2018.04.030.

Howcroft, W., Cartwright, I., Morgenstern, U., 2018. Mean transit times in headwater catchments: insights from the Otway Ranges, Australia. Hydrol. Earth Syst. Sci. 22, 635–653. https://doi.org/10.5194/hess-22-635-2018.

Hrachowitz, M., Savenije, H., Bogaard, T.A., Tetzlaff, D., Soulsby, C., 2013. What can flux tracking teach us about water age distribution patterns and their temporal dynamics? Hydrol. Earth Syst. Sci. 17, 533–564. https://doi.org/10.5194/hess-17-533-2013.

Hrachowitz, M., Soulsby, C., Tetzlaff, D., Malcolm, I.A., Schoups, G., 2010a. Gamma distribution models for transit time estimation in catchments: physical interpretation of parameters and implications for time-variant transit time assessment. Water Resour. Res. 46, W10536. https://doi.org/10.1029/2010WR009148.

Hrachowitz, M., Soulsby, C., Tetzlaff, D., Speed, M., 2010b. Catchment transit times and landscape controls-Does scale matter? Hydrol. Process. 24, 117–125. https://doi.org/ 10.1002/hyp.7510.

Hugenschmidt, C., Ingwersen, J., Sangchan, W., Sukvanachaikul, Y., Duffner, A., Uhlenbrook, S., Streck, T., 2014. A three-component hydrograph separation based on geochemical tracers in a tropical mountainous headwater catchment in northern Thailand. Hydrol. Earth Syst. Sci. 18, 525–537. https://doi.org/10.5194/hess-18525-2014.

Hollins, S.E., Hughes, C.E., Crawford, J., Cendón, D.I., Meredith, K.M., 2018. Rainfall isotope variations over the Australian continent – implications for hydrology and isoscape applications. Sci. Total Environ. 645, 630–645. https://doi.org/10.1016/j.scitotenv.2018.07.082.

International Atomic Energy Agency, 2017. Global Network of Isotopes in Precipitation. http://www.iaea.org/water.

Jones, J.A.A., 1997. Pipeflow contributing areas and runoff response. Hydrol. Process. 11, 35–41. https://doi.org/10.1016/j.jhydrol.2012.07.029.

Jones, J.A.A., 2004. Implications of natural soil piping for basin management in upland Britain. Land Degrad. Dev. 15, 325–349. https://doi.org/10.1002/ldr.618.

Jurgens, B.C., Bohlke, J.K., Eberts, S.M., 2012. TracerLPM (Version 1): an Excel® Workbook for Interpreting Groundwater Age Distributions from Environmental Tracer Data. U.S. Geological Survey Techniques and Methods Report 4-F3. pp. 60.

Kabeya, N., Katsuyama, M., Kawasaki, M., Ohte, N., Sugimoto, A., 2007. Estimation of mean residence times of subsurface waters using seasonal variation in deuterium excess in a small headwater catchment in Japan. Hydrol. Process. 21, 308–322. https://doi.org/10.1002/hyp.6231.

Kirchner, J.W., 2016. Aggregation in environmental systems-Part 1: seasonal tracer cycles quantify young water fractions, but not mean transit times, in spatially heterogeneous catchments. Hydrol. Earth Syst. Sci. 20, 279–297. https://doi.org/10.5194/hess-20279-2016.

Kirchner, J.W., Feng, X., Neal, C., 2000. Fractal stream chemistry and its implications for contaminant transport in catchments. Nature 403, 524–527. https://doi.org/10.1038/35000537.

Kite, G., 1989. An extension to the salt dilution method of measuring streamflow. Int. J. Water Resour. Dev. 5, 19–24. https://doi.org/10.1080/07900628908722408.

Lachassagne, P., Wyns, R., Dewandel, B., 2011. The fracture permeability of hard rock aquifers is due neither to tectonics, nor to unloading, but to weathering processes. Terra. Nova 23, 145–161. https://doi.org/10.1111/j.1365-3121.2011.00998.x.

Lee, K.S., Kim, J.M., Lee, D.R., Kim, Y., Lee, D., 2007. Analysis of water movement through an unsaturated soil zone in Jeju Island, Korea using stable oxygen and hydrogen isotopes. J. Hydrol. 345, 199–211. https://doi.org/10.1016/j.jhydrol.2007.08.006.

Maloszewski, P., 2000. Lumped-parameter Models as a Tool for Determining the Hydrological Parameters of Some Groundwater Systems Based on Isotope Data, vol. 262. IAHS-AISH Publication, pp. 271–276.

Maloszewski, P., Zuber, A., 1982. Determining the turnover time of groundwater systems with the aid of environmental tracers : 1. Models and their applicability. J. Hydrol. 57, 207–231. https://doi.org/10.1016/0022-1694(82)90147-0.

McCallum, J.L., Cook, P.G., Simmons, C.T., Werner, A.D., 2014. Bias of apparent tracer ages in heterogeneous environments. Ground Water 52, 239–250. https://doi.org/10. 1111/gwat.12052.

McDonnell, J.J., 1990. A rationale for old water discharge through macropores in a steep, humid catchment. Water Resour. Res. 26, 2821–2832. https://doi.org/10.1029/ WR026i011p02821.

McDonnell, J.J., Beven, K., 2014. Debates—the future of hydrological sciences: a (common) path forward? A call to action aimed at understanding velocities, celerities and residence time distributions of the headwater hydrograph. Water Resour. Res. 50, 5342–5350. https://doi.org/10.1002/2013WR015141.

McGuire, K.J., McDonnell, J.J., 2006. A review and evaluation of catchment transit time modeling. J. Hydrol. 330, 543–563. https://doi.org/10.1016/j.jhydrol.2006.04.020.

Menció, A., Folch, A., Mas-Pla, J., 2012. Identifying key parameters to differentiate groundwater flow systems using multifactorial analysis. J. Hydrol. 472, 301–313. https://doi.org/10.1016/j.jhydrol.2012.09.030.

Meyer, J.L., Strayer, D.L., Wallace, J.B., Eggert, S.L., Helfman, G.S., Leonard, N.E., 2007. The contribution of headwater streams to biodiversity in river networks. J. Am. Water Resour. Assoc. 43, 86–103. https://doi.org/10.1111/j.1752-1688.2007. 00008.x.

Morgenstern, U., Daughney, C.J., Leonard, G., Gordon, D., Donath, F.M., Reeves, R., 2015. Using groundwater age and hydrochemistry to understand sources and dynamics of nutrient contamination through the catchment into Lake Rotorua, New Zealand. Hydrol. Earth Syst. Sci. 19, 803–822. https://doi.org/10.5194/hess-19-8032015.

Morgenstern, U., Stewart, M.K., Stenger, R., 2010. Dating of streamwater using tritium in a post nuclear bomb pulse world: continuous variation of mean transit time with streamflow. Hydrol. Earth Syst. Sci. 14, 2289–2301. https://doi.org/10.5194/hess14-2289-2010.

Morgenstern, U., Taylor, C.B., 2009. Ultra low-level tritium measurement using electrolytic enrichment and LSC. Isot. Environ. Health Stud. 45, 96–117. https://doi.org/10.1080/10256010902931194.

Neklapilova, B., 2008a. Conductivity Measurements and Large Volumes Distillation of Samples for Tritium Analysis. ANSTO Internal Guideline, Technical Report ENV-i070-002. ANSTO – Institute for Environmental Research, Australia.

Neklapilova, B., 2008b. Electrolysis and Small Volume Distillation of Samples for Tritium Activity Analysis, ANSTO Internal Guideline, Technical Report ENV-i-070-003. ANSTO – Institute for Environmental Research, Australia.

Owuor, S.O., Butterbach-Bahl, K., Guzha, A.C., Rufino, M.C., Pelster, D.E., Díaz-Pinés, E., Breuer, L., 2016. Groundwater recharge rates and surface runoff response to land use and land cover changes in semi-arid environments. Ecol. Process. 5, 16. https://doi. org/10.1186/s13717-016-0060-6.

Parks Victoria, 2018. Great Otway National Park. http://parkweb.vic.gov.au/explore/ parks/great-otway-national-park.

Rice, K.C., Hornberger, G.M., 1998. Comparison of hydrochemical tracers to estimate source contributions to peak flow in a small, forested, headwater catchment. Water Resour. Res. 34, 1755–1766. https://doi.org/10.1029/98WR00917.

Sklash, M.G., Farvolden, R.N., 1979. The role of groundwater in storm runoff. J. Hydrol. 43, 45–65. https://doi.org/10.1016/S0167-5648(09)70009-7.

Sophocleous, M., 2002. Interactions between groundwater and surface water: the state of the science. Hydrogeol. J. 10, 52–67. https://doi.org/10.1007/s10040-001-0170-8. Soulsby, C., Malcolm, I.A., Youngson, A.F., Tetzlaff, D., Gibbins, C.N., Hannah, D.M., 2005. Groundwater-surface water interactions in upland Scottish rivers; hydrological, hydrochemical and ecological implications. Scot. J. Geol. 41, 39–49. https://doi.org/ 10.1144/sjg41010039.

Stewart, M.K., Morgenstern, U., Gusyev, M.A., Małoszewski, P., 2017. Aggregation effects on tritium-based mean transit times and young water fractions in spatially heterogeneous catchments and groundwater systems. Hydrol. Earth Syst. Sci. 21, 4615–4627. https://doi.org/10.5194/hess-21-4615-2017.

Stewart, M.K., Morgenstern, U., McDonnell, J.J., 2010. Truncation of stream residence time: how the use of stable isotopes has skewed our concept of streamwater age and origin. Hydrol. Process. 24, 1646–1659. https://doi.org/10.1002/hyp.7576.

Suckow, A., 2014. The age of groundwater–definitions, models and why we do not need this term. Appl. Geochem. 50, 222–230. https://doi.org/10.1016/j.apgeochem.2014.04.016.

Tadros, C.V., Hughes, C.E., Crawford, J., Hollins, S.E., Chisari, R., 2014. Tritium in Australian precipitation: a 50 year record. J. Hydrol. 513, 262–273. https://doi.org/ 10.1016/j.jhydrol.2014.03.031.

Tetzlaff, D., Soulsby, C., 2008. Sources of baseflow in larger catchments - using tracers to develop a holistic understanding of runoff generation. J. Hydrol. 359, 287–302. https://doi.org/10.1016/j.jhydrol.2008.07.008.

Tweed, S.O., Weaver, T.R., Cartwright, I., 2005. Distinguishing groundwater flow paths in different fractured-rock aquifers using groundwater chemistry: Dandenong Ranges, southeast Australia. Hydrogeol. J. 13, 771–786. https://doi.org/10.1007/s10040004-0348-y.

Uchida, T., Kosugi, K., Mizuyama, T., 1999. Runoff characteristics of pipeflow and effects of pipeflow on rainfall-runoff phenomena in a mountainous watershed. J. Hydrol. 222, 18–36. https://doi.org/10.1016/S0022-1694(99)00090-6.

Uchida, T., Tromp-van Meerveld, I., McDonnell, J.J., 2005. The role of lateral pipe flow in hillslope runoff response: an intercomparison of non-linear hillslope response. J. Hydrol. 311, 117–133. https://doi.org/10.1016/j.jhydrol.2005.01.012.

Uhlenbrook, S., Frey, M., Leibundgut, C., Maloszewski, P., 2002. Hydrograph separations in a mesoscale mountainous basin at event and seasonal timescales. Water Resour. Res. 38, 311–3114. https://doi.org/10.1029/2001WR000938.

Uhlenbrook, S., Hoeg, S., 2003. Quantifying uncertainties in tracer-based hydrograph separations: a case study for two-, three- and five-component hydrograph separations in a mountainous catchment. Hydrol. Process. 17, 431–453. https://doi.org/10.1002/hyp.1134.

van Verseveld, W.J., Barnard, H.R., Graham, C.B., McDonnell, J.J., Brooks, J.R., Weiler, M., 2017. A sprinkling experiment to quantify celerity–velocity differences at the hillslope scale. Hydrol. Earth Syst. Sci. 21, 5891–5910. https://doi.org/10.5194/ hess-21-5891-2017.

Williams, G., 2004. The Gellibrand River: balancing environmental and urban water demand in a climate of change. In: Proceedings of the International River Symposium, pp. 15.

Winter, T.C., 1995. Recent advances in understanding the interaction of groundwater and surface water. Rev. Geophys. 33, 985–994. https://doi.org/10.1029/95RG00115.

Zhang, Z.Q., Evaristo, J., Li, Z., Si, B.C., McDonnell, J.J., 2017. Tritium analysis shows apple trees may be transpiring water several decades old. Hydrol. Process. 31, 1196–1201. https://doi.org/10.1002/hyp.11108.

Zuber, A., Witczak, S., Rozanski, K., Sliwka, I., Opoka, M., Mochalski, P., Kuc, T., Karlikowska, J., Kania, J., Jackowicz-Korczynski, M., Dulinski, M., 2005. Groundwater dating with ^{3}H and SF_6 in relation to mixing patterns, transport modelling and hydrochemistry. Hydrol. Process. 19, 2247–2275. https://doi.org/10.1002/hyp.5669.